Trends in Analytical Chemistry 160 (2023) 116981

Contents lists available at ScienceDirect

Trends in Analytical Chemistry

journal homepage: www.elsevier.com/locate/trac

Early detection of tumour-associated antigens: Assessment of point-of-care electrochemical immunoassays

Mihaela Puiu [a, b], Cristina Nativi [c], Camelia Bala [a, b, *]

[a] R&D Center LaborQ, University of Bucharest, 4-12 Regina Elisabeta Blvd., 030018, Bucharest, Romania
[b] Department of Analytical Chemistry & Physical Chemistry, University of Bucharest, 4-12 Regina Elisabeta Blvd., 030018, Bucharest, Romania
[c] Department of Chemistry "Ugo Schiff", University of Florence, Via Della Lastruccia, 3-13, I-50019, Sesto F.no (FI), Italy

ARTICLE INFO

Article history:
Received 31 December 2022
Received in revised form
24 January 2023
Accepted 9 February 2023
Available online 10 February 2023

Keywords:
Tumour-associated antigens
Electrochemical immunoassay
Organic-inorganic hetero-nano-interfaces
Early detection
Signal amplification
Magnetic nanoparticles

ABSTRACT

The development of highly sensitive and selective platforms for cancer biomarkers detection plays a crucial for early diagnosis, monitoring disease progression, and subsequent cancer treatment. Among various types of biomarkers, tumour-associated antigens (TAAs) that are expressed *via* tumours, are targeted for early detection in point-of-care (POC) locations. In this review, a brief introduction of the most important TAAs and their application in the recognition of different types and stages of cancer will be passed into, along with a detailed assessment of electrochemical bio/immunosensors designed for TAA detection in POC environments. The detection of small fragments of TAAs such as the tumour-associated carbohydrate antigens (TACAs) may provide a rapid, accurate and cost-effective tool to complete the clinical picture. Multiplexing capabilities, signal amplification strategies and ultimately, the feasibility of organic−inorganic hetero-nano-interfaces -based bio/immunosensors for POC applications will be critically discussed.

1. Introduction

Cancer has become a life-threatening and widespread disease, representing the outcome of complex epigenetic and/or genomic abnormalities through different stages of cell development. Monitoring cancer progression through the early stages of evolution is crucial for developing effective treatment strategies. During a tumour progression, overexpression of genes (DNA, mRNA), proteins or saccharides generally occurs. These aberrant events are accompanied by the formation, at the preclinical phase, of neo-antigens which have been recognized as biomarkers diagnostically precious to detect tumoral events before the advent of noticeable symptoms [1,2]. The term "biomarker" designates a broad range of biochemical entities, such as sugars, lipids, proteins, nucleic acids, small metabolites, cytogenetic and cytokinetic parameters, as well as entire tumour cells found in body fluids or tumour tissues [3]. Among various types of biomarkers, tumour antigens (TA) are expressed *via* tumours and are applied in the scanning and diagnosis of cancer. TAs encompass two classes of biomarkers: a) tumour-associated antigens (TAAs, overexpressed by tumours compared to normal tissues) and b) tumour-specific antigens (TSAs, specific for a particular tumour and overexpressed just by cancerous cells) [2]. TAAs are critical to the rational development of medical diagnosis and therapeutics because closely related to the onset, prognosis, and recurrence of cancer. Most cancer biomarkers are glycoconjugates abnormally- or over-expressed on the surface of malignant cells and whose detection can be directed against either the protein/ceramide portion or the glycan moiety separately [4]. Mammalian cells surface are surrounded by a thick coating of carbohydrates covalently linked, through N- and O-glycosidic linkages [5,6], to proteins (glycoproteins), lipids (glycolipids) ceramides (glycosphingolipids) [7]. In cancer, the glycosylation processes, regulated by glycosyl transferases and glycosidases, play a pivotal role in the development of malignancy. In this context, special attention shall be devoted to glycosylation processes. And forming the so-called glycocalix. Abnormal glycosylation is not easily predicted and may occur at the onset and/or during tumour progression, leading to the exposure of neo-glycans termed tumour-associated carbohydrate antigens (TACAs) [8]. Generally, in humans glycosylation is based on the combination of ten monosaccharides: glucose (Glc), galactose (Gal),

* Corresponding author. Department of Analytical Chemistry & Physical Chemistry, University of Bucharest, 4-12 Regina Elisabeta Blvd., 030018, Bucharest, Romania.
E-mail address: camelia.bala@chimie.unibuc.ro (C. Bala).

https://doi.org/10.1016/j.trac.2023.116981
0165-9936/

List of abbreviations:

AAO	Anodic aluminium oxide
ACAC	acetylacetone
AFP	alpha-fetoprotein
Aq	anthraquinone-2-carboxylic acid
AuNP	gold nanoparticle
AuNS	gold nanostars
ASA	acetylsalicylic acid
CA	cancer antigen
CD	carbon dots
CEA	carcino-embryonic antigen
CLIA	chemiluminescence immunoassay
CNT	carbon nanotube
COF	covalent organic framework
CRC	colorectal cancer, chitosan CS
CV	cyclic voltammetry
DETA	diethylenetriamine
DPV	differential pulse voltammetry
Dva	1,4-benzenedicarboxaldehyde
EIS	electrochemical impedance spectroscopy
ESCC	oesophageal squamous cell carcinoma
ECL	electrochemiluminescence
ELISA	enzyme-linked immunosorbent assay
Fc	ferrocene carboxylic acid
FET	field effect transistor, Fuc fucose
Gal	galactose
GalNAc	N-acetylgalactosamine
GCE	glassy carbon electrode
Glc	glucose
GlcNAc	N-acetylglucosamine
GO	graphene oxide
GOx	glucose oxidase
GR	graphene
HCC	hepatocellular carcinoma
H-diamond	Hydrogen-terminated diamond
FISH	fluorescent in-situ hybridization
HRP	horseradish peroxidase
HSP	heat shock protein, LFIA lateral flow immunoassay
LOD	limit of detection
Man	mannose
MB	magnetic beads
MCH	6-mercapto-1-hexanol
MIP	molecularly imprinted polymer
MOF	metal-organic framework
MUC1	mucin 1
MUC4	mucin 4
MS	mass spectrometry
NE	norepinephrine
Neu5Ac	N-acetylneuraminic acid
OIHNI	organic−inorganic hetero-nano-interfaces
O-GalNAc	*O*-linked N-acetylgalactosamine
NSCLC	non-small cell lung cancer
OSCC	oral squamous cell carcinoma
PANI	polyaniline
PCa	prostate cancer
PCR	Polymerase Chain Reaction
PEC	photoelectrochemistry
PNIPAM	poly(N-isopropylacrylamide)
POC	point-of-care
PSA	polypeptide-specific antigen
PSMA	poly(styrene-alt-maleic anhydride)
rGO	reduced graphene oxide
RIA	radioimmune assay
sLe^A	sialyl-Lewis A
SERS	Surface-enhanced Raman scattering
SGFET	solution-gate field-effect transistor
Ser	serine
SPE	screen printed electrode
SPR	surface plasmon resonance
Tn	Thomsen-nouvelle antigen
SWV	square wave voltammetry
TA	tumour antigen
TAA	tumour associated antigen
TACA	tumour associated carbohydrate antigen
TFPB	1,3,5-tris (p-formylphenyl) benzene
STn	sialyl Thomsen-nouvelle antigen
Thr	threonine
TPS	tissue polypeptide-specific antigen
TSA	tumour specific antigen
WE	working electrode, Xyl xylose

N-acetylglucosamine (GlcNAc), N-acetylgalactosamine (GalNAc), glucuronic acid, iduronic acid, fucose (Fuc), mannose (Man), xylose (Xyl) and N-acetyl neuraminic acid (Neu5Ac) (Fig. 1) [9]. The monosaccharide composition, the type of glycosidic bonds as well as the 3D carbohydrate conformation affect the antigenic properties of the resulting glycoside and, consequently, the immune response elicited.

Among the number of subtypes of biomarkers, biomarkers for diagnostic and prognosis applications evolved considerably with the advent of the precision medicine. Indeed, such biomarkers can successfully be used to identify people with a disease but also to classify the disease [10,11]. A selection of relevant tumour biomarkers and their applications in cancer diagnosis/prognosis are summarized in Table 1.

2. Glycoconjugate biomarkers

Glycans are almost ubiquitous in biological systems [12] and are deputed to a plethora of roles, including cancer progression. Glycosylation is one of the most abundant protein post-translational modifications and over half of all human proteins are glycosylated. A major category of glycosylation concerns the mucin-type-*O*-glycans occurring on secreted and *trans*-membrane mucin glycoproteins [7]. Under physiological conditions, the biosynthesis of *O*-glycans produces extended, highly branched oligosaccharides, while in pathological situations *O*-glycans are truncated and the over-simplified GalNAc-a-Ser/Thr (Tn antigen) and its sialylated form Neu5Aca2, 6GalNAc-a-Ser/Thr (sialyl Tn or STn antigen) are formed (Fig. 1). Tn and STn antigens have been detected in almost every human carcinoma cancer type [13] and are over expressed in breast, colon, lung, pancreatic, and prostate tumours [14]. Since it has largely been shown that Tn and STn antigens are associated with the pathogenesis of these diseases, at present Tn, STn and TACAs in general, are considered useful human cancer biomarkers [15] to target in diagnostics.

TACAs' detection is usually achieved by means of chromatographic techniques coupled with mass spectrometry (MS) [6]. The procedure requires glycoproteins' extraction from serum or plasma

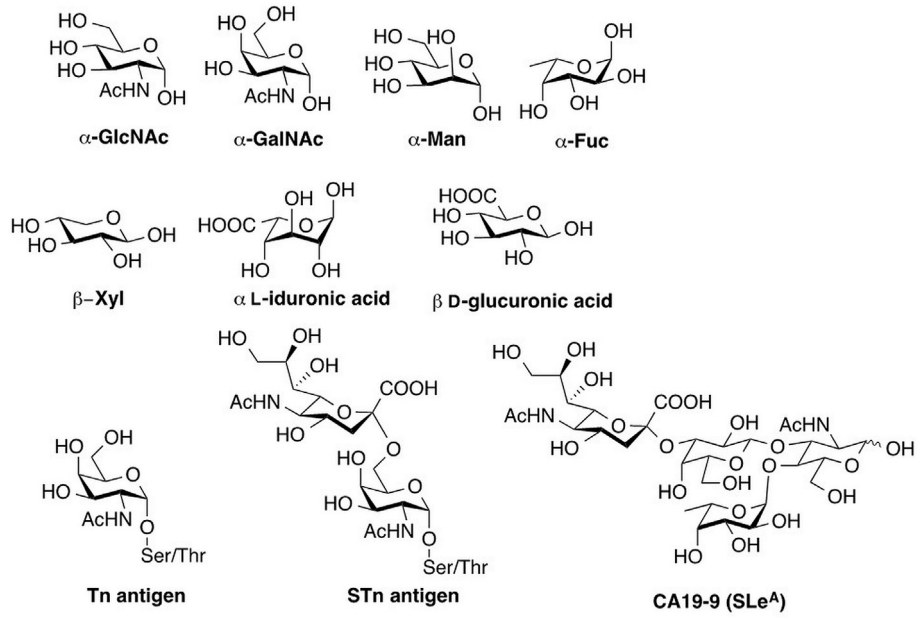

Fig. 1. Structure of Tn, STn and CA19-9 TACAs and of common monosaccharides part of TACAs.

Table 1
Tumour-associated antigens and their applications to different stages of cancer diagnosis. Adapted from Ref. [10] with permission of Wiley.

Markers	Full name	Applications	Type of malignancy
HSPs	Heat shock proteins	Prognosis	PCa/bladder cancer/NSCLC/melanoma/CRC
AFP	Alpha-fetoprotein	Early diagnosis/monitoring	HCC/gastric cancer
CEA	Carcino-embryonic antigen	Early diagnosis/prognosis	CRC/lung cancer/gastric cancer
CA50	Carbohydrate antigen 50	Diagnosis/prognosis	Gastric cancer/pancreatic cancer
CA19-9	Carbohydrate antigen 19-9	Diagnosis/prognosis	Gastric cancer/CRC/pancreatic cancer
CA125	Carbohydrate antigen 125	Diagnosis/prognosis	Ovarian cancer/endometrial cancer/gastric cancer
CA549	Carbohydrate antigen 549	Diagnosis	Breast cancer
CA724	Carbohydrate antigen 724	Diagnosis	Ovarian cancer/gastric caner
MUC1 (CA15-3)	Mucin1	Prognosis	NSCLC
MUC4	Mucin4	Prognosis	Pancreatic cancer
GPC3	Glypican-3	Diagnosis/prognosis	HCC
SCCA	Squamous cell carcinoma antigen	Early diagnosis	HCC/cervical cancer/NSCLC/ESCC
TPS	Tissue polypeptide-specific antigen	Diagnosis/monitoring	Pancreatic cancer/CRC/bronchial cancer/OSCC/breast cancer
PSA	Prostate-specific antigen	Early diagnosis/screening/prognosis	PCa

NSCLC, non-small cell lung cancer; CRC, colorectal cancer; HCC, hepatocellular carcinoma; ESCC, oesophageal squamous cell carcinoma; OSCC, oral squamous cell carcinoma; PCa, prostate cancer.

and affinity enrichment/purification steps, based on antibody- or lectin interactions [16]. Glycans are then removed from the peptide backbone by chemical or enzymatic protocols. The resulted glycans are further enriched through hydrophilic interaction chromatography or solid phase extraction, enabling a separation based on their structure polarity and size. Thus, native state MS analysis can be performed directly, although glycans may be further subjected to derivatization (*i.e.,* permethylation or acetylation) [5,6]. Other reported techniques for the detection of cancer biomarkers are enzyme-linked immunosorbent assay (ELISA) [17], Polymerase Chain Reaction (PCR) [18], chemiluminescence immunoassay (CLIA) [19], radioimmune assays (RIA) [20], lateral flow immunoassay (LFIA) [19] and fluorescent in-situ hybridization (FISH) [21].

By contrast, biosensors are devices that provide specific quantitative or semi-quantitative information about analytes by simply attaching a biological recognition element to a transducer [22] and recording the changes in the biosensor's output signal following either a specific binding interaction or an enzyme-catalysed reaction. Thus, affinity-based biosensors rely mostly on the pairing of specific biomolecules (antibodies, aptamers, nucleic acids, or peptides) with a broad range of analytes, while in enzyme-catalysed systems, the analyte undergoes a chemical transformation [22,23]. TAAs can be detected by means of TACA affinity interaction with anti-TACA/TAA antibodies in two immunoaffinity-formats, as depicted in Scheme 1.

A) direct binding or indirect competitive assays with surface immobilized TACAs targeting the corresponding anti-TAA/TACA antibodies, and
B) direct binding and direct competitive assays with surface-immobilized antibodies targeting TAAs/TACAs from samples.

However, the implementation of these formats on immunosensing platforms designed for point-of-care (POC) applications meets several challenges such as poor operational stability, high costs and limited sensitivity. On the other hand, the electrochemical biosensors are best suited to function in POC locations, due to their simplicity, low-cost, fast response, high sensitivity, selectivity and finally, miniaturization capabilities [24]. A cost-effective alternative is to replace TACAs with synthetic low

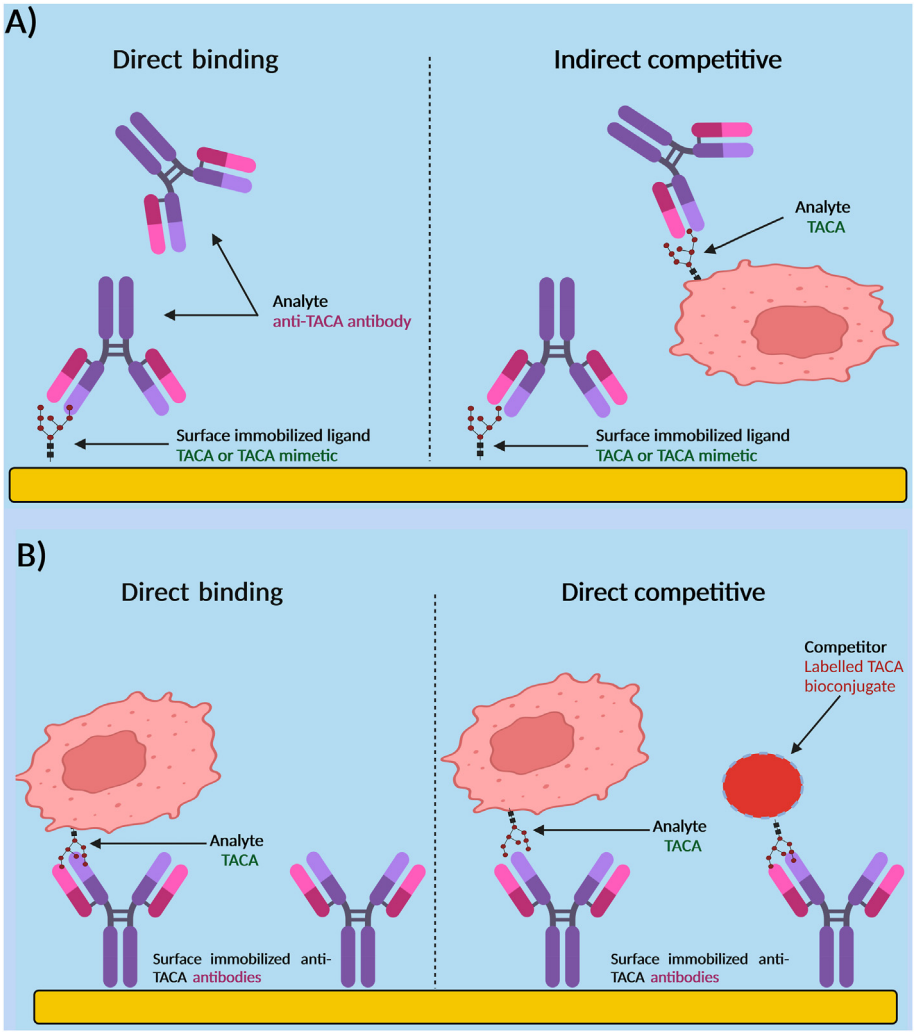

Scheme 1. Main immunoassay formats for TAA/TACA detection: A) with surface-immobilized TACA ligand targeting anti-TACA antibody (direct binding) or anti-TACA antibody in the presence of TACA (indirect competitive format) and B) with surface-immobilized anti-TACA antibody targeting TACA (direct binding) or TACA in the presence of a TACA -labelled (enzymatic, fluorescent, redox, radioisotopic) bioconjugate. Created with BioRender.com.

molecular weight analogues or mimetics, resulted from the conjugation of the TACA mimetic to a peptide carrier containing established T-cell epitope [25,26]. These compounds are stable in ambient conditions, and they can be easily immobilized onto surfaces *via* simple covalent binding. The use TACA mimetics for the detection anti-TACA antibodies is still in infancy and there are few works reporting TACA-based immunosensors [27,28]. In this review we will provide a restricted selection of the most significant electrochemical immunosensors for TAAs detection that either use TACA mimetics or report assay formats in which TAAs can be replaced by TACA mimetics. The latest advances in multiplexing capabilities, signal amplification strategies and development of conductive interfaces will be critically discussed.

3. Trending electrochemical methods for TAAs detection. Development of conductive interfaces

Most electrochemical strategies for cancer biomarker detection exploit affinity assays combined with various voltametric techniques such as cyclic voltammetry (CV) [29], square wave voltammetry (SWV) [27,30,31], differential pulse voltammetry (DPV) [32,33], electrochemical impedance spectroscopy (EIS) [34,35], amperometry [36,37], electrochemiluminescence (ECL) [38] and potentiometry (*e.g.* field effect transistor (FET) [39]), these making them ideal candidates for point-of-care diagnostics. Also, photoelectrochemistry (PEC) has been applied in the detection of cancer biomarkers [35].

The voltametric/amperometric sensing techniques operate by applying a voltage as input signal and measuring the current as output signal. The current is generated by a redox event occurring at the working electrode and is limited by the mass transfer rate of the electroactive species from the bulk solution to the electrode interface [40]. In amperometry, direct current is measured by applying a constant potential to the working electrode (WE). The plot of current *vs.* time is recorded as the electrode reactions evolve under constant potential [41]. The current change is a measure of the electron transfer rate and is proportional to the concentration of the analyte [42]. During a CV experiment, the potential of WE is linearly scanned *vs.* time (forward and then backward to the initial potential) in the presence of a redox probe [43]. In DPV, a succession of pulses with a fixed small amplitude on a linear potential ramp is applied to WE and superimposed on the slowly changing base potential. In SWV, the staircase potential ramp is modified with square-shaped potential pulses (forward and reverse) [44].

SWV has the ability to operate at high frequencies which minimise the depletion of electroactive species, by comparison to other pulse techniques [45]. EIS is a technique used mostly to detect interfacial modification of electrodes. EIS uses an amplitude sinusoidal AC excitation signal, typically in the range of 2–10 mV, to determine measurable resistance and capacitance changes following the adsorption/deposition of materials on the electrode surface. Thus, the resistance and capacitance of the electric double-layer change cause variation in the electrochemical impedance. ECL is a process involving light emission by species electrogenerated at electrodes when they are undergoing highly energetic electron-transfer reactions and forming excited states [46]. ECL is initiated and regulated by the application of a proper potential at electrode surface, thus allowing control on the time and position of the light-emitting reactions and providing excellent reproducibility and sensitivity. The FET-based sensors operate by means of an electrical field modulating charge carriers across a semiconductor material [47]. The semiconductor determines the type of charge carriers; thus the current flow can be either the result of movement of holes ("p-type"), or electrons ("n-type"). In a typical FET configuration, the electric current flows along a semiconductor channel connected to the source and drain electrodes [48]. The third electrode (the gate contact) is capacitively coupled to the device through a thin dielectric layer (typically SiO_2); the gate modulates the conductance between these two electrodes. A FET-based sensor detects potential changes on its gate surface, that are the result of the binding of probe molecules [45,48]. In order to design operative electrochemical sensing interfaces, attention must be paid to two integrated components: (a) bio-recognition elements that interact specific with the target analyte causing observable changes at the sensor's surface and (b) signal transducers, that create measurable signals following the specific interactions occurring at the electrode's surface [49]. Thus, changes in the electron transfer rate, surface conductivity, electrode potential following electrode modification play a crucial role in sensor's performance characteristics [50].

In recent years, various types of nanomaterials and nanocomposites have emerged as promising tools for biomarkers detection, provided that they exhibit well-defined structures, suitable physico-chemical characteristics, and good biocompatibility [51]: carbon-based nanomaterials, *e.g.* carbon nanotubes (CNT) [52], graphene (GR) [53], carbon dots (CD) [38], nanodiamonds [54]), conductive polymers, noble metals (silver and gold), magnetic nanoparticles, metal–organic frameworks (MOFs) and peptide molecular wires [27,34,55]. By modifying the electrode surface, as signal transducers, they provide the advantages of high signal amplification, multi-functionality, easy preparation and increased thermal stability [56]. More recently, organic–inorganic hetero-nano-interfaces (OIHNIs) have been applied to electrode modification to increase the sensitivity, selectivity, and the detection rate [57]. OIHNIs are spongy crystal-like materials consisting of metal nodes (metal clusters or ions) and polymeric nanomaterials/ligands that display intrinsic properties, such as high surface-to-volume ratio, high porosity, increased absorbability, and

Table 2
Selected bio/immunosensing platforms amenable for POC applications.

Platform	TAA biomarker	Capturing element/assay protocol	Electrochemical technique	Sample fluid	LOD/linear range	Signal amplifier system	Pros for POC applications	Ref.
AuNP/rGO/SPE	CA15-3	Anti-CA15-3 antibody/ Sandwich assay	SWV	Human serum, artificial saliva	0.08 fg/mL/ 0.1 fg/mL – 1 μg/mL	HRP/H_2O_2/ hydroquinone (HQ)	Rapid screening Stability Low LOD Wide linear range Suitable for early diagnosis/monitoring	[30]
2D-covalent organic frameworks (COF)/1,3,5-tris (p-formylphenyl) benzene (TFPB)/1,4-benzenedicarboxaldehyde (Dva)/GCE	CEA	Anti-CEA antibody/ Sandwich assay	DPV	Buffer (pH 7.0)	0.034 ng/mL 0.11 ng/ mL –80 ng/ mL	(COF)/ Thionine (Thi)/ AuNPs	Stability High specificity High selectivity	[33]
Hydrogen-terminated diamond (H-diamond) solution-gate field-effect transistor (SGFET)	CA19-9	Anti CA19-9/ Direct binding	SGFET	Buffer (pH 7.0)	0.001 U/mL 0.001–1000 U/mL	–	High specificity Few operational steps Suitable for early diagnosis	[68]
CdS/Chitosan/graphitic carbon nitride $-C_3N_4$/ GCE	PSA	DNA aptamer/ complementary base pairing	ECL	Serum	0.14 pg/mL 1 pg/ mL –100 ng/ mL	–	High sensitivity Easy operation Suitable for early diagnosis/monitoring	[69]
Anodic aluminium oxide (AAO) membrane-based nanochannels with magnetically controlled transport of hydrophilic ferrofluids	CA15-3	Anti-CA15-3 antibody/Direct binding	DPV	1:10 diluted serum samples	0.0013 U/mL 0.01 U/ mL –100 U/ mL	–	Rapid detection Excellent selectivity Amenable to multiplexing	[70]
Au/SPE	CEA	Anti-CEA antibody/ Sandwich assay	Dual EIS/Surface-enhanced Raman scattering (SERS)	Bovine serum	Not reported 0.25 –250 ng/ mL(EIS) Not reported 0.025 ng/mL - 250 ng/mL (SERS)	Gold nanostars (AuNS)	Sensitive response at concentrations within the physiological level Capability for multiplexing	[71]

enhanced electrocatalytic efficiency [58]. Different metal oxides and bimetallic nanomaterials functionalized with various polymers such as polyaniline (PANI) [59], polythiophene [60], chitosan (CS) [61], have been implemented on platforms for electrochemical detection of biomarkers; nanocomposites based on non-metallic nanoparticles (graphene, graphene oxide (GO) along with metal oxides/sulphides such as cerium oxide (CeO_2) [62,63] cobalt oxide (Co_3O_4) [64], iron oxide (Fe_3O_4) [61,65,66], cobalt sulphide (CoS_2) [28]), have been used to develop electrochemical immunosensors for TAA biomarkers. A list dedicated the most recent and relevant works that exploit OIHNIs capabilities as conductive coating supports for surface modifications and signal enhancers is presented in Table 2.

3.1. Metal oxide/bimetallic based organic–inorganic hetero-nano-interfaces

Metal organic frameworks (MOFs) are crystalline porous materials with periodic network structure; MOFs are formed by connecting metal ions (or clusters) and bridging organic ligands through self-assembly [67]. The synergistic effects of the dynamics of analyte transport (within MOF) and high loading capacity (due to a high volume-to surface-area ratio) contribute to the enhanced sensitivity of MOFs. In the past decade, various metal oxides, such as CuO, ZnO, NiO, Co_3O_4, and Fe_2O_3, were synthesized by calcining their corresponding MOFs [62]. The derivatives of MOFs have been employed as substrates for electrochemical biosensors, due to their large specific surface area, excellent biocompatibility, and superior electrochemical performance [55].

Bimetallic nanoparticles composed of two different metal elements display often better sensing characteristics than their monometallic counterparts. For example, a mixed valence state of Ce-MOF and Fe-MOF possess excellent catalytic activity, suitable for electrochemical detection of small biomolecules [72]. A label-free electrochemical immunosensor based on MOF derivatives was developed for the detection of CA19-9 by Wang and collab [62]. Bimetallic cerium and ferric oxide nanoparticles embedded within mesoporous carbon matrix (represented by CeO_2/FeOx@mC500) were obtained from the bimetallic CeFe-based metal organic framework (CeFe-MOF) by calcination at 500 °C. The CA19–9 antibody was anchored to the CeO_2/FeOx@mC network through chemical absorption between carboxylic groups of antibodies and CeO_2 or FeOx by ester-like bridging. Fe_2O_3 improved the conductive properties of the transducer, while the formed graphitized layer with porous structure increased the specific surface area. The binding of CA19-9 to the MOF-anchored anti-CA19-9 antibody increased the charge transfer resistance of the electrode/solution interface, monitored through EIS measurements. The EIS based immunosensor exhibited an extremely low detection limit of 10 μU/mL within a dynamic range from 0.1 mU/mL to 10 U/mL toward CA 19–9. It also illustrated excellent specificity, good reproducibility and stability, and acceptable application for serum samples, 100-fold diluted with 0.01 M PBS solution (pH 7.4) and spiked with different amounts of CA19-9.

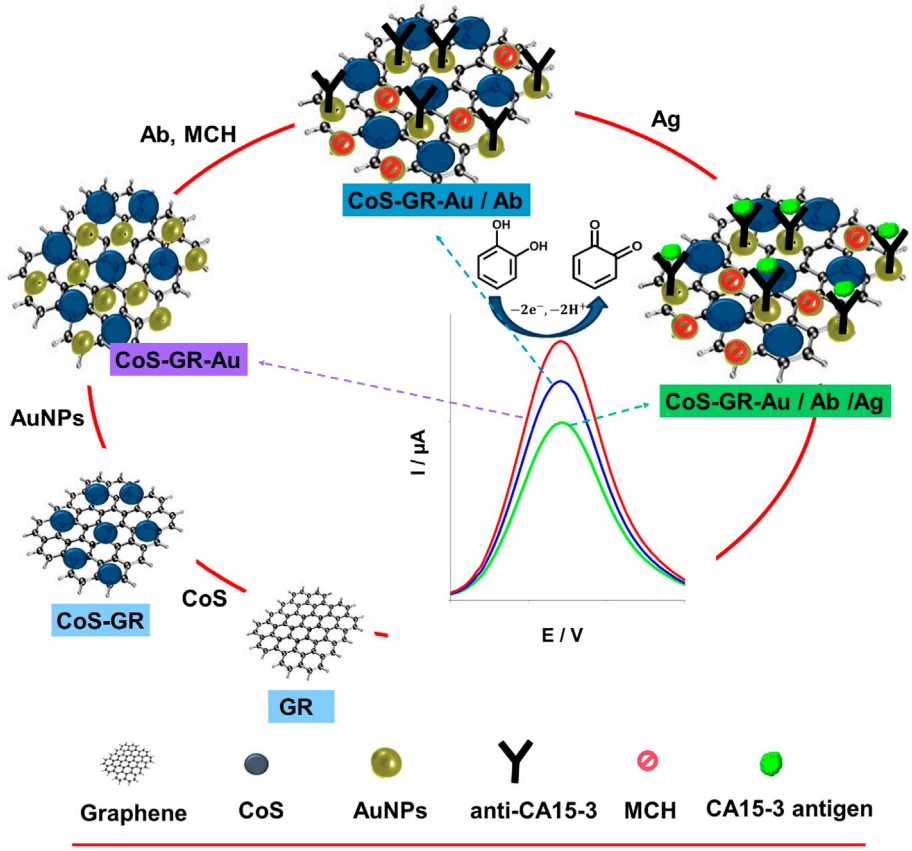

Fig. 2. Development and detection principle of the CoS_2-GR-AuNPs/Ab/SPE immunosensor. First, the CoS_2-GR nanocomposite suspension was dropped onto the screen-printed working electrode surface. Then, the formation of AuNPs on the CoS_2-GR/SPE was carried out by successive CV scanning between the range potential of −0.2 and + 1.6 V in $HAuCl_4/H_2SO_4$ solution. The immobilization of anti-CA15-3 Ab succeeded, followed by the addition of a blocking agent, 6-mercapto-1-hexanol (MCH). The DPV response decreased along with the increase of CA15-3 antigen (Ag) concentration towards the oxidation of catechol which is due to the formation Ab/Ag complex onto surface; the interfacial electron transfer was considerably prevented, causing the decrease of the DPV current. Reproduced from Ref. [28] with permission of Elsevier.

3.2. Graphene - and graphene organic–inorganic hetero-nano-interfaces based immunosensors for TAA

Graphene has attracted considerable interest in fundamental and applied research due to its peculiar 2D hexagonal nano-structure that confers superior thermal and electrical conductivity, mechanical strength, chemical stability, and remarkable charge carrier mobility [73,74]. Aromaticity in graphene is local, two π-electrons being delocalized over every hexagon ring. Graphene is hydrophobic, and chemically inert. Graphene oxide and reduced graphene oxide (rGO) are the oxidized forms of graphene [75]. GO is less electrically conductive, but high soluble in water; on the other hand, rGO is less dispersible in water or other solvents, but displays significant electrical conductivity. The presence of oxygen containing groups (hydroxyl: −OH, epoxide, carboxyl: >C═O, and carboxylic acid: −COOH) over the basal plane of GN is responsible for the high solubility of GO in water and also for the ability of binding upon the interfacial area of graphene of various bio-molecules such as enzymes, antibodies and DNA [76].

An electrochemical OIHNIS platform based on CoS_2-GR and AuNPs composites (CoS_2-GR-AuNPs) was developed by Khoshroo and co-workers for the detection of carbohydrate antigen 15−3 (CA15-3, or Mucin 1) [28]. AuNPs were used to increase the surface area available for antibody binding (Fig. 2). CoS_2-GR nanocomposite displayed electro-catalytic activity toward the oxidation of catechol, providing further a large surface area, and increasing the amount of immobilized anti-CA15-3 antibody (Ab). The fabricated immunosensor exhibited a linear range of 0.1−150 U/mL and a low detection limit (LOD) of 0.03 U/mL. The immunosensor displayed good accuracy, stability, specificity, and it was successfully applied for CA15-3 detection in serum samples.

3.3. Strategies for signal amplification

Basically, most signal amplification strategies operate by increasing the loading capacity of capture antibody and the upload of electrochemical tags. Sandwich-type immunosensor is a widely used model in the electrochemical immunosensors [77].

An interesting sandwich-type electrochemical immunosensor has been fabricated for the simultaneous determination of three

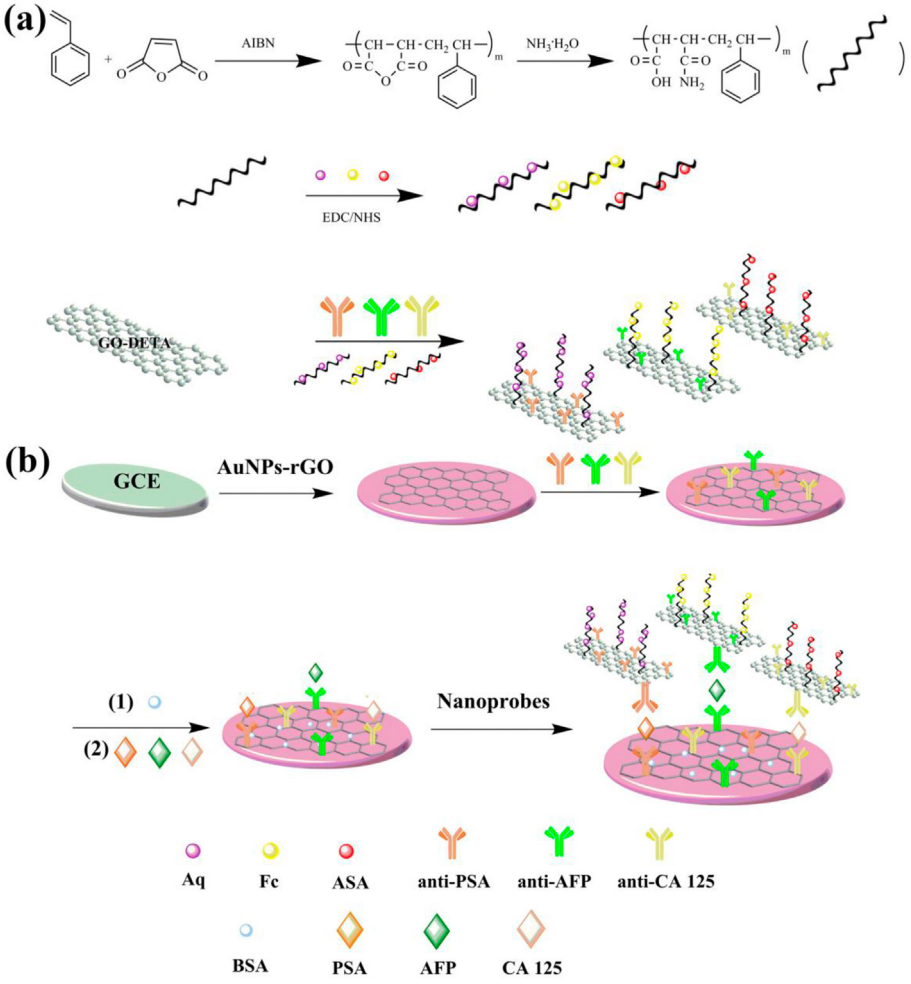

Fig. 3. Signal amplification in the multiplexed electrochemical immunoassay (a) Preparation and assembly of nanoprobe: PSMA was hydrolyzed by $NH_3 \cdot H_2O$ for the generation of NH_2-PSMA-COOH. After activation of the carboxyl groups, the three signal molecules ferrocenecarboxylic acid (Fc), anthraquinone-2-carboxylic acid (Aq), and acetylsalicylic acid (ASA) were assembled on the surface of NH_2-PSMA-COOH, respectively. Then, diethylenetriamine modified GO (GO-DETA) was used to separately load different secondary antibodies (Ab_2) to synthesize GO-Ab_2 probes. Finally, the active carboxyl group of PSMA-Fc (or PSMA-Aq, PSMA-ASA) and the amino group of GO were used for the amidation reaction to get the final nanoprobe with both signal molecule and Ab_2. (b) Fabrication and assembly of the electrochemical immunosensor the glassy carbon electrode was modified with a reduced graphene oxide (rGO)/AuNPs to immobilize capture antibodies. The target antigens ASA, PSA and CA125, are first captured onto (rGO)/AuNPs modified surface. The binding of the nanoprobe loaded with the secondary antibodies caused an increase of the DPV current directly proportional with the antigen concentration Reproduced from Ref. [78] with permission of Elsevier.

TAAs [78].

The signal-amplifying platform was assisted by GO loaded with poly(styrene-alt-maleic anhydride) (PSMA). PSA, AFP and CA125 were employed as model test molecules (Fig. 3). This sandwich-type immunoassay could detect the three antigens in a single DPV scan. The multiplexed immunosensor displayed a wide linear range (1.13 pg/mL - 113 ng/for PSA, 0.35 pg/mL - 35 ng/mLfor AFP and 0.025 U/mL - 250 U/mL for CA 125. LODs were 86 fg/mL, 14 fg/mL, and 0.0019 U/mL for PSA, AFP, and CA 125, respectively. This strategy provides a simple and sensitive method for the identification and validation of specific early cancer [78].

As mentioned above, GO has the advantage of high loading capacity and good conductivity. On the other hand, bimetallic/metal oxides nanomaterials display catalytic activity. Various catalyst are introduced to amplify the electrochemical signal in Fenton and Fenton-like reactions: Fe_3O_4, iron-based hydrogel, MOFs, hemin, ferrous reagent and other iron-free catalysts like Cu_2O_2 [67]. Other catalysts containing metal ions like Fe^{3+}, Cu^{2+} and Co^{2+} were classified as Fenton-like catalysts because they catalyse H_2O_2 decomposition to produce •OH.

A sandwich electrochemical sensor was constructed based on the degradation of Methylene Blue through Fenton reaction, initiated by Fe-MIL-88B—NH_2 (Fe-MOF). The AuNP on the surface of Fe-MOF were used to bind the labelled antibody (Ab_2). Fe-MOF can catalyse the generation of •OH by its own peroxidase-like activity and thus degrading the thin layer of Methylene Blue which was covered by Au-rGO nanocomposites (with coating antibody (Ab_1). The modification of Au-rGO on the substrate increases the electron transfer on electrode surface. The remained MB from the surface becomes oxidized thereby generating a current signal. SWV was used to quantify PSA. The immunoassay was stable, specific and reproducible, with a LOD of 0.13 pg/mL and an analytical range from 0.001 to 100 n/mL [79].

Another, sandwich-type electrochemical immunosensor was able to rapidly detect CA15-3 with an ultra-low LOD of 0.08 fg/mL within a wide linear concentration range from 0.1 fg/mL to 1 μg/mL Here copper-based metal-organic framework (Cu-MOF) conjugate with glucose oxidase (GOx) and CA15-3 secondary antibody (Ab_2) were used as immunoprobes, to recognize CA15-3, and to initiate radical polymerization *via* cascade catalytic reaction. Upon introduction of immunoprobes, GOx catalyses glucose oxidation to produce H_2O_2; H_2O_2 is subsequently catalysed by Cu-MOF to react with acetylacetone (ACAC) and result in ACAC radicals for the in-situ formation of poly(N-isopropylacrylamide) (PNIPAM) on the substrate. Due to the poor conductivity, the formed PNIPAM hinders the charge transfer of $[Fe(CN)_6]^{3-/4-}$ strongly increasing the resistance difference. The immunosensor can be incorporated into future POC devices to determine CA15-3 in in blood and saliva samples [34].

Magnetic immunosensors use magnetic beads (MBs) coated with ligand able to sense in magnetic field. Among magnetic nanoparticles, iron oxides and in particular magnetite (Fe_3O_4) and its oxidized form maghemite (γ-Fe_2O_3) have attracted much attention due to their biocompatibility, low toxicity, and ease of preparation at low cost [80]. An important challenge for the affinity-based sensors is electrode fouling when the sensor is interrogated in real sample (human blood/serum sample/or cell matrix). Capturing specific proteins in real samples using magnetic beads is one of feasible approach for reducing the non-specific binding [29]. The functional core of the MB is coated with non-magnetic polymeric materials and can be used for immobilizing antibodies in an immunoassay. The magnetization of MBs will be zero in the absence of any magnetic field while the MBs become paramagnetic under the influence of applied magnetic field. An aptamer-antibody hybrid immunosensor integrated with a magnetic bead capturing system for the detection of CA125 in human

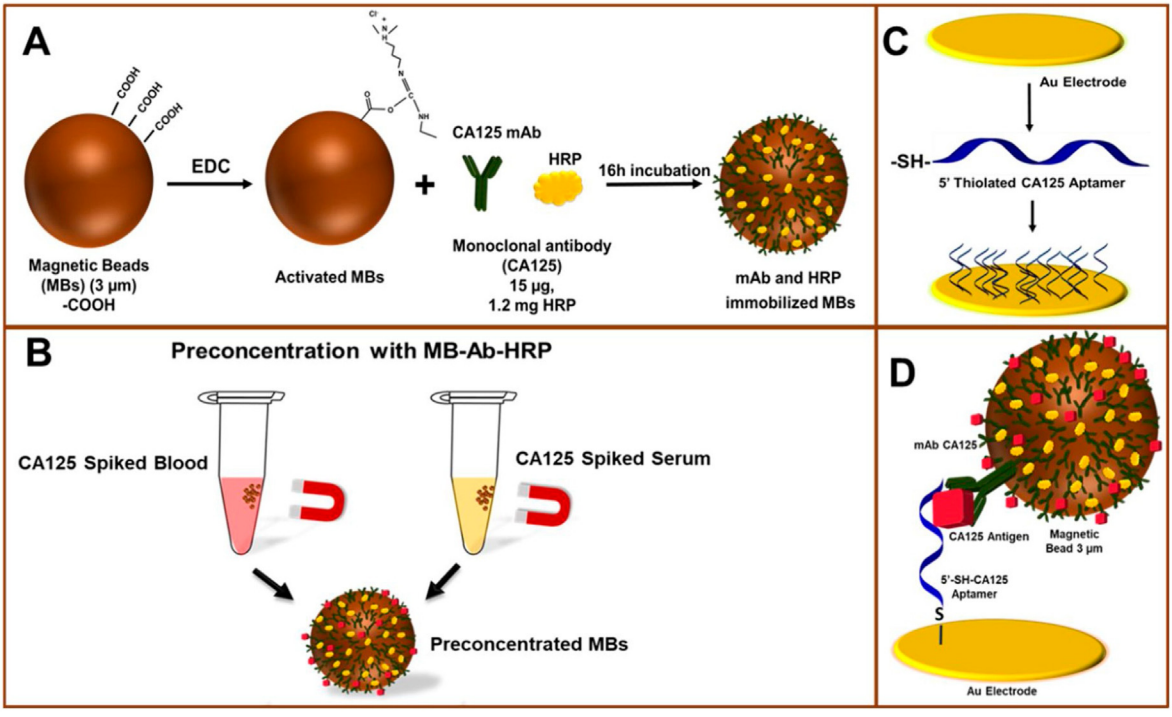

Fig. 4. Representation of dual-bioreceptor immunoassay development. Immobilization of antibodies and enzyme tags onto the MBs (A), preconcentration and isolation of CA125 from human serum and blood samples using antibodies conjugated MBs (B), immobilization of thiolated aptamers onto the gold electrode surfaces (C), and formation of sandwich immunocomplex using dual-receptor immunosensor (D). Reproduced from Ref. [29] with permission of Elsevier.

blood and serum was reported by Sadasivam and collab [29]. To prevent electrode fouling from interfering blood proteins, CA125 in human blood/serum samples were specifically captured and transferred to the electrode using monoclonal antibodies conjugated magnetic beads. Two different electrochemical approaches were used to monitor the immuno-complex formation for CA125 detection: one that exploited the electrocatalytic activity of the signalling enzyme (horseradish peroxidase, HRP) conjugated to MBs and the other, utilized an external redox probe in the solution (here, potassium hexacyanoferrate) (Fig. 4). The formation of the sandwich immunocomplex aptamer/CA125/anti-CA125 antibody/HRP caused a) a current increase, due to the electrocatalytic response of MB-integrated enzyme with its substrate, H_2O_2. Monitored through amperometry and b) an increase of the charge transfer resistance monitored through EIS measurements. In human serum samples, a sensitivity of 0.017 mA/U mL and LOD of 0.08 U/mL was achieved. The immunosensor was able to detect CA125 levels with a broad clinical range of 2 U/mL to 100 U/mL using monoclonal antibodies immobilized on magnetic beads (MBs).

3.4. Implementation of TACA mimetics for supporting multiplexing capability

There are two main issues to be addressed for achieving high sensitivity-multiplexed detection. Firstly, the content of biomarkers is extremely low in samples collected from patients at an early stage of disease [81]. Secondly, different redox probes with distinguishable and independent electrochemical signals are required [78]. One promising approach is the use of TACA mimetics immobilized onto redox -labelled peptide molecular wires [27]. Here the redox reporter (Methylene Blue) was directly attached to the peptide-based conductive support. The TACA mimetic was further immobilized at the end of the peptide wire. Then, the fabricated sensor was interrogated against the anti-TACA antibody. The antibody binding to the immobilized antigen caused a sharp decreasing of the SWV signal. This affinity format allowed the electrochemical detection of the antibody with a LOD of 180 ng/mL and is amenable to indirect competitive formats designed for multiplexed microarray platforms. Another promising approach has recently reported on the replacement of anti-TACA antibodies with an innovative class of Molecularly Imprinted Polymers (MIPs), or “plastic Abs”, based on norepinephrine (NE) [82]. The MIP-based platform was able to recognize small entities of Tn antigen in a direct binding assay. The affinity pair was implemented on a surface plasmon resonance (SPR) chip, yet the assay format can be adapted for electrochemical detection.

4. Conclusions and perspectives

In this review, we have comprehensively focused on recent advances in the design of affinity-based electrochemical immunosensors for the early detection of TAA and TACA biomarkers. Many analytical devices and protocols were set for simultaneous detection of multiple TAA, aiming at increased sample throughput, reduced measurement time and less sample depletion. Moreover, microfluidics-based lab-on-chip devices open the gates for multiplexed, miniaturized, and high throughput detection. These portable and inexpensive platforms can provide both low LOD and increased sensitivity, especially when various approaches for signal amplification are used. The use of nanomaterials and nanocomposites to increase electroactive surface and ligand loading may bring to the fore some difficulties such as low selectivity, slow binding kinetics due to the heterogeneous interfaces, and non-specific binding of the target present in complex biological samples. OIHNI-based bio/immunosensors have gained ground continuously in the past decade due to their high loading capability of antibodies, enzymes and aptamers and assistance against biomolecules’ degradation. For example, MOFs possess characteristic porous features and consequently large surface areas able to anchor large molecules, electroactive species or MNPs. Furthermore, MOFs interconnected pore structures ensure effective mass transfer through diffusion at the electrode surface. Some drawbacks still exist, since iron-based MOFs display poor conductivity, and their use may limit the electron transfer through MOF-modified electrodes. Finally, biomolecules labelled with magnetic nanoparticles will be magnetically driven to be retained on a surface, effects that can be exploited for signal enhancement in sandwich immunoassays. The use of catalysts immobilized on magnetic beads for both catalytic and separation processes will provide additional assets in the development of microfluidic platforms with electrochemical detection. The detection of small fragments of TAAs, TACAs (or TACA mimetics) in indirect competitive formats may provide a rapid, accurate and cost-effective tool to complete the clinical picture for early-stage diagnosis.

C. Bala proposed the subject, drafted, and revised manuscript. C. Nativi drafted and revised manuscript. M. Puiu analysed references, drafted and revised the manuscript. All authors read and approved the manuscript.

Declaration of competing interest

The authors declare the following financial interests/personal relationships which may be considered as potential competing interests: BALA Camelia reports financial support was provided by Romanian Government Ministry of Research Innovation and Digitization.

Data availability

No data was used for the research described in the article.

Acknowledgement

This work was supported by a grant from the Romanian Ministry of Research, Innovation and Digitization, CNCS/CCCDI—UEFISCDI, project no PN—III—P4-ID-PCE2020-0998, within PNCDI III. The authors acknowledge the networking support from COST Action CA18132- Functional Glyconanomaterials for the Development of Diagnostics and Targeted Therapeutic Probes (GlycoNanoProbes), supported by COST (European Cooperation in Science and Technology).

References

[1] R. Laocharoensuk, Electroanalysis 28 (2016) 1716.
[2] S. Hassanpour, M. Hasanzadeh, Microchem. J. 168 (2021), 106424.
[3] L. Wu, X. Qu, Chem. Soc. Rev. 44 (2015) 2963.
[4] O.M.T. Pearce, Glycobiology 28 (2018) 670.
[5] M.J. Kailemia, D. Park, C.B. Lebrilla, Anal. Bioanal. Chem. 409 (2017) 395.
[6] C. Sorieul, F. Papi, F. Carboni, S. Pecetta, S. Phogat, R. Adamo, Pharmacol. Ther. 235 (2022), 108158.
[7] D. Bapu, J. Runions, M. Kadhim, S.A. Brooks, Cancer Lett. 375 (2016) 367.
[8] E. Meeusen, E. Lim, S. Mathivanan, Proteomics 17 (2017), 1600442.
[9] K. Kappler, T. Hennet, Gene Immun. 21 (2020) 224.
[10] C.C. Liu, H. Yang, R. Zhang, J.J. Zhao, D.J. Hao, Eur. J. Cancer Care 26 (2017), e12446.
[11] R.M. Califf, Exp. Biol. Med. 243 (2018) 213.
[12] C.R. Bertozzi, Kiessling, L. Laura, Science 291 (2001) 2357.
[13] V. da Costa, T. Freire, Cancers 14 (2022) 1854.
[14] M. Balmaña, A. Sarrats, E. Llop, S. Barrabés, R. Saldova, M.J. Ferri, J. Figueras, E. Fort, R. de Llorens, P.M. Rudd, R. Peracaula, Clin. Chim. Acta 442 (2015) 56.
[15] T. Ju, Y. Wang, R.P. Aryal, S.D. Lehoux, X. Ding, M.R. Kudelka, C. Cutler, J. Zeng, J. Wang, X. Sun, J. Heimburg-Molinaro, D.F. Smith, R.D. Cummings, Proteonomics Clin. Appl. 7 (2013) 618.
[16] J. Zhao, D.M. Simeone, D. Heidt, M.A. Anderson, D.M. Lubman, J. Proteome Res.

5 (2006) 1792.
[17] Y.S. Wang, S.F. Ren, W. Jiang, J.Q. Lu, X.Y. Zhang, X.P. Li, R. Cao, C.J. Xu, Ann. Transl. Med. 9 (2021) 788.
[18] M.S. Tabatabaei, R. Islam, M. Ahmed, Anal. Chim. Acta 1143 (2021) 250.
[19] H. Sohrabi, N. Bolandi, A. Hemmati, S. Eyvazi, S. Ghasemzadeh, B. Baradaran, F. Oroojalian, M. Reza Majidi, M. de la Guardia, A. Mokhtarzadeh, Microchem. J. 177 (2022), 107248.
[20] P. Lakhera, V. Chaudhary, A. Jha, R. Singh, P. Kush, P. Kumar, Mater. Today Chem. 26 (2022), 101129.
[21] L. Li, D. Feng, J. Zhao, Z. Guo, Y. Zhang, RSC Adv. 5 (2015), 105992.
[22] D. Sadighbayan, K. Sadighbayan, M.R. Tohid-kia, A.Y. Khosroushahi, M. Hasanzadeh, Trends Anal. Chem. 118 (2019) 73.
[23] N.J. Ronkainen, H.B. Halsall, W.R. Heineman, Chem. Soc. Rev. 39 (2010) 1747.
[24] R.-E. Munteanu, P.S. Moreno, M. Bramini, S. Gáspár, Anal. Bioanal. Chem. 413 (2021) 701.
[25] D. Feng, A.S. Shaikh, F. Wang, ACS Chem. Biol. 11 (2016) 850.
[26] C. Nativi, F. Papi, S. Roelens, Chem. Commun. (J. Chem. Soc. Sect. D) 55 (2019) 7729.
[27] M. Puiu, L.-G. Zamfir, G.M. Danila, F. Papi, C. Nativi, V. Mirceski, C. Bala, Sensor. Actuator. B Chem. 345 (2021), 130416.
[28] A. Khoshroo, M. Mazloum-Ardakani, M. Forat-Yazdi, Sensor. Actuator. B Chem. 255 (2018) 580.
[29] M. Sadasivam, A. Sakthivel, N. Nagesh, S. Hansda, M. Veerapandian, S. Alwarappan, P. Manickam, Sensor. Actuator. B Chem. 312 (2020), 127985.
[30] T.S. Martins, J.L. Bott-Neto, O.N. Oliveira, S.A.S. Machado, Microchim. Acta 189 (2021) 38.
[31] Z. Tang, Y. Fu, Z. Ma, Biosens. Bioelectron. 91 (2017) 299.
[32] Y. Xie, X. Zhi, H. Su, K. Wang, Z. Yan, N. He, J. Zhang, D. Chen, D. Cui, Nanoscale Res. Lett. 10 (2015) 477.
[33] H. Liang, Y. Luo, Y. Li, Y. Song, L. Wang, Anal. Chem. 94 (2022) 5352.
[34] C. Zhang, D. Zhang, Z. Ma, H. Han, Biosens. Bioelectron. 137 (2019) 1.
[35] J. Peng, Z. Zheng, H. Tan, J. Yang, D. Zheng, Y. Song, F. Lu, Y. Chen, W. Gao, Sensor. Actuator. B Chem. 363 (2022), 131863.
[36] Y. Xu, H. Wang, J. Electroanal. Chem. 915 (2022), 116333.
[37] B.S. Munge, A.L. Coffey, J.M. Doucette, B.K. Somba, R. Malhotra, V. Patel, J.S. Gutkind, J.F. Rusling, Angew. Chem., Int. Ed. 50 (2011) 7915.
[38] M. Zou, Y. Gong, X. Sun, C. Ding, Sensor. Actuator. B Chem. 369 (2022), 132330.
[39] L. Zhou, K. Wang, H. Sun, S. Zhao, X. Chen, D. Qian, H. Mao, J. Zhao, Nano-Micro Lett. 11 (2019) 20.
[40] L. Jing, C. Xie, Q. Li, M. Yang, S. Li, H. Li, F. Xia, Anal. Chem. 94 (2022) 269.
[41] W. Zhang, G. Xiao, J. Chen, L. Wang, Q. Hu, J. Wu, W. Zhang, M. Song, J. Qiao, C. Xu, Anal. Bioanal. Chem. 413 (2021) 2407.
[42] J. Rojas, A. Fontana Tachon, D. Chevalier, T. Noguer, J.L. Marty, C. Ghommidh, Sensor. Actuator. B Chem. 102 (2004) 284.
[43] M. Labib, E.H. Sargent, S.O. Kelley, Chem. Rev. 116 (2016) 9001.
[44] V. Mirceski, L. Stojanov, R. Gulaboski, J. Electroanal. Chem. 872 (2020), 114384.
[45] K. Malecka, E. Mikuła, E.E. Ferapontova, Sensors 21 (2021).
[46] Y. Chen, S. Zhou, L. Li, J.-j. Zhu, Nano Today 12 (2017) 98.
[47] A.C.A.U. De Moraes, T.T.I.C. Kubota Lauro, Chemosensors 4 (2016) 20.
[48] M. Kaisti, Biosens. Bioelectron. 98 (2017) 437.
[49] P.V.V. Romanholo, C.A. Razzino, P.A. Raymundo-Pereira, T.M. Prado, S.A.S. Machado, L.F. Sgobbi, Biosens. Bioelectron. 185 (2021), 113242.
[50] N. Sun, H. Yu, H. Wu, X. Shen, C. Deng, Trends Anal. Chem. 135 (2021), 116168.
[51] M. Pirsaheb, S. Mohammadi, A. Salimi, Trends Anal. Chem. 115 (2019) 83.
[52] S. Rashid, M.H. Nawaz, I.u. Rehman, A. Hayat, J.L. Marty, Sensor. Actuator. B Chem. 330 (2021), 129351.
[53] Y. Wu, P. Xue, K.M. Hui, Y. Kang, Biosens. Bioelectron. 52 (2014) 180.
[54] C. Wang, J. Li, M. Kang, X. Huang, Y. Liu, N. Zhou, Z. Zhang, Anal. Chim. Acta 1141 (2021) 110.
[55] M. Wang, M. Hu, Z. Li, L. He, Y. Song, Q. Jia, Z. Zhang, M. Du, Biosens. Bioelectron. 142 (2019), 111536.
[56] S. Zhang, F. Rong, C. Guo, F. Duan, L. He, M. Wang, Z. Zhang, M. Kang, M. Du, Coord. Chem. Rev. 439 (2021), 213948.
[57] S. Kempahanumakkagari, K. Vellingiri, A. Deep, E.E. Kwon, N. Bolan, K.-H. Kim, Coord. Chem. Rev. 357 (2018) 105.
[58] P.K. Kalambate, J. Noiphung, N. Rodthongkum, N. Larpant, P. Thirabowonkitphithan, T. Rojanarata, M. Hasan, Y. Huang, W. Laiwattanapaisal, Trends Anal. Chem. 143 (2021), 116403.
[59] R. Salahandish, A. Ghaffarinejad, E. Omidinia, H. Zargartalebi, K. Majidzadeh-A, S.M. Naghib, A. Sanati-Nezhad, Biosens. Bioelectron. 120 (2018) 129.
[60] S. Kumar, S. Kumar, S. Srivastava, B.K. Yadav, S.H. Lee, J.G. Sharma, D.C. Doval, B.D. Malhotra, Biosens. Bioelectron. 73 (2015) 114.
[61] D. Peng, R.-P. Liang, H. Huang, J.-D. Qiu, J. Electroanal. Chem. 761 (2016) 112.
[62] M. Wang, M. Hu, B. Hu, C. Guo, Y. Song, Q. Jia, L. He, Z. Zhang, S. Fang, Biosens. Bioelectron. 135 (2019) 22.
[63] N. Pachauri, K. Dave, A. Dinda, P.R. Solanki, J. Mater. Chem. B 6 (2018) 3000.
[64] L. Liu, S. Choi, J. Power Sources 348 (2017) 138.
[65] A.A. Ansari, B.D. Malhotra, Coord. Chem. Rev. 452 (2022), 214282.
[66] B. Dou, L. Xu, B. Jiang, R. Yuan, Y. Xiang, Anal. Chem. 91 (2019), 10792.
[67] J. Feng, C. Chu, Z. Ma, Electrochem. Commun. 125 (2021), 106970.
[68] B. Xu, Q. Zhang, X. Chang, D. Zhang, G. Chen, S. He, Y. Wang, Y. Feng, H.-X. Wang, Mater. Lett. 318 (2022), 132116.
[69] B. Huang, X.-P. Liu, J.-S. Chen, C.-j. Mao, H.-L. Niu, B.-K. Jin, Microchim. Acta 187 (2020) 155.
[70] J. Jiao, H. Zhang, J. Zheng, Biosens. Bioelectron. 201 (2022), 113963.
[71] Y. Castaño-Guerrero, F.T.C. Moreira, A. Sousa-Castillo, M.A. Correa-Duarte, M.G.F. Sales, Electrochim. Acta 366 (2021), 137377.
[72] B. Peng, J. Cui, Y. Wang, J. Liu, H. Zheng, L. Jin, X. Zhang, Y. Zhang, Y. Wu, Nanoscale 10 (2018) 1939.
[73] S.A. Zaidi, F. Shahzad, S. Batool, Talanta 210 (2020), 120669.
[74] M. Yusuf, M. Kumar, M.A. Khan, M. Sillanpää, H. Arafat, Adv. Colloid Interface Sci. 273 (2019), 102036.
[75] F. Arshad, F. Nabi, S. Iqbal, R.H. Khan, Colloids Surf., B 212 (2022), 112356.
[76] D. Ozkan-Ariksoysal, Biosensors 12 (2022).
[77] L. Jiao, Z. Mu, C. Zhu, Q. Wei, H. Li, D. Du, Y. Lin, Sensor. Actuator. B Chem. 231 (2016) 513.
[78] N. Wang, J. Wang, X. Zhao, H. Chen, H. Xu, L. Bai, W. Wang, H. Yang, D. Wei, B. Yuan, Talanta 226 (2021), 122133.
[79] J. Feng, H. Wang, Z. Ma, Microchim. Acta 187 (2020) 95.
[80] T. Jamshaid, E.T.T. Neto, M.M. Eissa, N. Zine, M.H. Kunita, A.E. El-Salhi, A. Elaissari, Trends Anal. Chem. 79 (2016) 344.
[81] Z. Liu, S. Lei, L. Zou, G. Li, L. Xu, B. Ye, Biosens. Bioelectron. 131 (2019) 113.
[82] P. Palladino, F. Papi, M. Minunni, C. Nativi, S. Scarano, ChemPlusChem 87 (2022), e202200068.